2011 IEEE/RSJ International Conference on
Intelligent Robots and Systems
September 25-30, 2011. San Francisco, CA, USA

A Bimanual Teleoperated System for Endonasal Skull Base Surgery

Jessica Burgner, *Member, IEEE*, Philip J. Swaney, *Student Member, IEEE*,
D. Caleb Rucker, *Member, IEEE*, Hunter B. Gilbert, Scott T. Nill, Paul T. Russell III, Kyle D. Weaver,
and Robert J. Webster III, *Member, IEEE*

***Abstract*— We describe transnasal skull base surgery, including the current clinical procedure and the ways in which a robotic system has the potential to enhance the current standard of care. The available workspace is characterized by segmenting medical images and reconstructing the available 3D geometry. We then describe thin, "tentacle-like" robotic tools with shafts constructed from concentric tube robots, and an actuation unit designed to robotically control them in a teleoperated setting. Lastly, we discuss the results of a proof-of-concept study in a cadaveric specimen, illustrating the ability of the robot to access clinically relevant skull base targets.**

I. INTRODUCTION

Since the first surgical needle was aimed by a robot at a location in a human brain [1], robotic surgical systems have been increasingly applied in medical applications [2], [3]. The recent commercial success of the da Vinci system has propelled teleoperated surgical assistant systems into the general knowledge base of surgeons and patients, establishing robots as standard tools for certain surgical procedures (e.g. radical prostatectomy).

Current trends in robot design are toward more refined and versatile laparoscopic robot systems [4], [5], and toward customized systems purpose-built for specific kinds of surgery that require smaller tools (e.g. [6]) and/or enhanced dexterity inside the patient (e.g. [7]). Systems have recently been introduced specifically for middle ear surgery [6], throat surgery [7], and single port abdominal surgery [8], among others. Many of these systems involve the use of various kinds of actuated, flexible, curved tool shafts that enable dexterous access to the surgical site without requiring the large open spaces necessary for straight tools that must pivot around the body entry point.

In this paper we describe a new teleoperated robotic system with miniature, tentacle-like tool shafts, which is customized for transnasal endoscopic skull base surgery. Our system is motivated by a number of recent attempts to use the da Vinci system for surgical procedures in the head and neck [9], [4], [10], primarily using transoral access. The skull base has even been accessed transorally [11], [12]. However, use of the da Vinci to access the skull base through the mouth violates the "keyhole" principle in surgery (i.e. that the smallest and least invasive entry channel that permits adequate access should be employed), because the nose is the most direct and least invasive natural orifice through which skull base access is possible. Nevertheless, these results are a testament to the ingenuity of surgeons in adapting robots for applications never foreseen by robot designers. They also clearly underscore the need for new purpose-designed systems for accessing the skull base, such as the one we describe in this paper.

Some prior results exist on use of robotic systems to aid in bone drilling to open access paths to the skull base [13], [14], [15]. There has also been research on robotic assistance of endoscope manipulation [16]. All of these prior results are complementary to our current system, which is designed to be deployed after the access channel has been created by bone drilling or other manual procedures, and which will work in conjunction with an endoscope.

In our system we use tentacle-like concentric-tube continuum robots (also called active cannulas) [17], [18], [19] as tool shafts. These consist of precurved concentric tubes made of superelastic nitinol, and have diameters comparable to surgical needles (usually 1-2 mm, although they can easily be made smaller or larger – nitinol tubes are available in stock diameters as small as 200 μm). The curve of the active cannula inside the patient can be controlled by axially rotating and translating each tube at its base. Mechanics-based models exist for these robots that can accommodate an arbitrary number of tubes, with general precurved shapes in free space [20], [18] and under external loads [19].

II. ENDOSCOPIC SURGERY AT THE SKULL BASE

The skull base is the most inferior part of the skull, dividing the intracranial structures including the brain, from the facial compartment which includes the sinuses. Neurovascular structures enter and exit the brain through the skull base, making surgery at this location challenging. Skull base surgery is currently evolving from traditional transfacial and transcranial approaches to the less invasive endoscopic endonasal approach [21].

A. Medical Motivation for Transnasal Skull Base Surgery

Tumors arising at the skull base are common. For example, tumors at the pituitary gland account for 15-20% of all

The authors thank Jonathan Forbes and Jason Ridley for assistance with cadaver experiments. This work was supported in part by National Institutes of Health grant R21 EB011628, and in part by the National Science Foundation grants 0651803 and award IIS-1054331.

J. Burgner, P.J. Swaney, D.C. Rucker, H.B. Gilbert, S.T. Nill, and R.J. Webster are with the Department of Mechanical Engineering, Vanderbilt University, Nashville, USA {jessica.burgner, robert.webster}@vanderbilt.edu

P.T. Russell and R.J. Webster are with the Department of Otolaryngology, Vanderbilt University Medical Center, Nashville, USA, paul.t.russell@vanderbilt.edu

K.D. Weaver is with the Department of Neurological Surgery, Vanderbilt University Medical Center, Nashville, USA, kyle.weaver@vanderbilt.edu

primary brain tumors [22], but are fortunately almost always benign. Depending on their location and size, such tumors can cause hormonal abnormalities, visual impairment or loss, headaches, etc. The American Brain Tumor Association states that 10-20% of the general population have a pituitary tumor [22], though many may not even realize it because these are slow-growing tumors.

Traditionally, surgery at the anterior, middle and posterior skull base requires complex transcranial or transfacial access [23]. However, these open procedures imply high risks for the patient and long recovery times. Advancements in manual (i.e. non-robotic) surgical instrument design have enabled transnasal minimally invasive techniques, resulting in significantly less trauma, fewer complications and shorter operation times [24], [21].

B. State of the Art in Skull Base Surgery

Endoscopic techniques and instruments can be used to safely and effectively approach and resect tumors of the pituitary gland in humans [25], [26]. The anatomy and endonasal approach are depicted in Fig. 1. The surgery begins with a widening of the nasal passage, in order to permit access to the anterior wall of the sphenoid sinus. An endoscope is then inserted from the nostril towards the sphenoid sinus passing the inferior and middle nasal turbinates. The sphenoid sinus is then exposed, marking the extent of the intranasal dissection. Resection of the posterior wall of the sphenoid allows subsequent incision of the dura and removal of the tumor.

The current instruments available to the surgeon to perform these operations are hand-held tools with a straight shaft and functional tip (dissectors, curettes, etc.) and various kinds of forceps (vascular forceps, scissors, etc.). These are manipulated using visual feedback from an operating microscope and/or an endoscope. The latter can be classified into four types for neuroendoscopy: (1) rigid fiberscopes, (2) rigid rod-lens endoscopes, (3) flexible endoscopes, and (4) steerable fiberscopes [23].

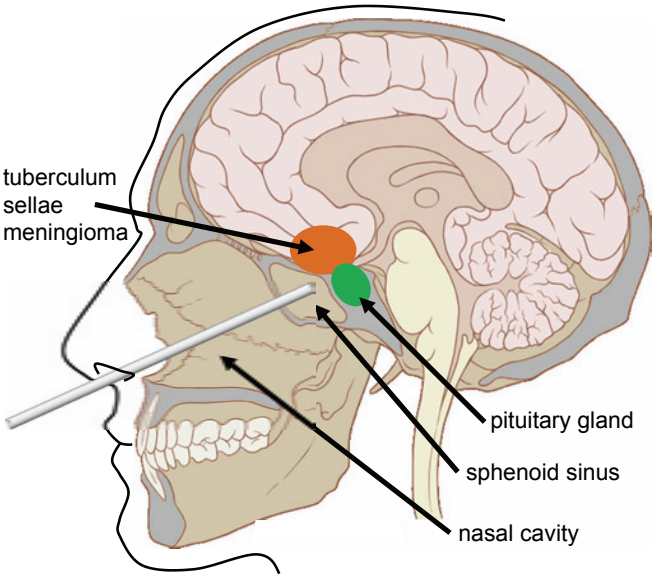

Fig. 1: Endonasal approach to the pituitary gland using a straight tool. The nasal cavity has to be prepared in order to gain access through the sphenoid sinus. Regions where tuberculum sellae meningiomas occur are almost inaccessible endonasally with current surgical tools.

Image guidance systems are also sometimes employed during the surgery. These systems (e.g. BrainLab, Medtronic, Inc.) allow registration of the intraoperative anatomy and tools with the preoperative medical images. One challenge in using these systems is that since surface-based registration is applied, there is a significant risk of clinically-relevant inaccuracy at the skull base [27], [28].

C. Motivation for a Robotic Approach

A robotic approach to skull base surgery that utilizes tentacle-like tools is motivated by a number of factors. First of all, not every pathology of the skull base is a candidate for a minimally invasive transnasal approach, because some are inaccessible to straight tools. For example, tuberculum sellae meningiomas (see Fig. 1) which are located above and in front of the pituitary gland at the skull base, have to be accessed transcranially. Only a few experimental procedures have been performed endonasally by expert surgeons in carefully selected patients [29]. Uniformly, surgeons conclude that better surgical instrumentation and visualization are needed in skull base procedures. Tentacle-like curved tools may permit less invasive access to the skull base, requiring less healthy sinus tissue to be removed. Tools that can "turn corners" may enable improved angles of approach to desired clinical targets. A steerable endoscope can similarly improve visualization by providing new viewpoints for the surgeon.

A robotic system can also assist with tool management, a significant challenge in transnasal skull base surgery. Preventing inadvertent collisions between instruments (a.k.a. the "sword fighting" effect) could enable surgery to proceed more safely, smoothly, and rapidly. It would also reduce the surgeon's cognitive load, enabling him/her to be concerned only with the tips of instruments, without having to maintain a mental 3D model of the entire shaft of all instruments at all times.

A robotic system can also be directly connected to an image guidance system and assist the surgeon with navigation and identification of intraoperative structures and pathology. This can be done either via overlaying image data on the endoscope image, or by actively using this data to apply virtual fixtures [30].

Lastly a robotic system can improve the ergonomics of the operation for the surgeon. Standing beside the patient and reaching over the patient to manipulate tools inserted through the nose often requires contortions from the physician that cause fatigue, and in some cases may not be conducive to long-term neck and back health. In contrast, placing the surgeon in a seated position at a comfortable console will reduce fatigue and improve ergonomics.

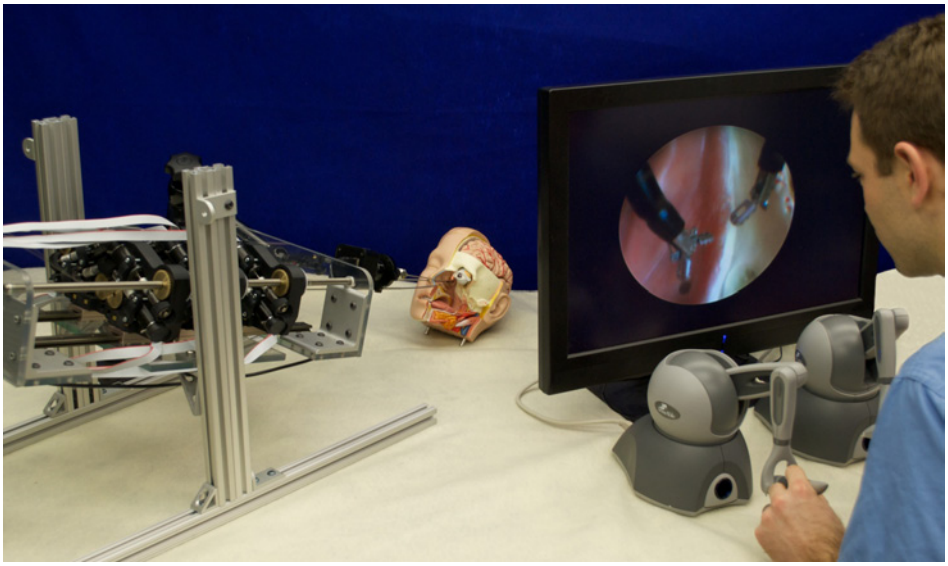

Fig. 2: Prototype bimanual teleoperated active cannula system for endonasal skull base surgery. The robot on the left actuates two three-tube cannulas, which are inserted through the nose into a head model. An endoscope held by a passive arm provides the view for the master console (right). The two cannulas are teleoperated with two haptic devices.

III. SYSTEM DESIGN

To address the challenges of minimally invasive skull base surgery, we designed and constructed a prototype bimanual teleoperated system. The complete system is depicted in Fig. 2. It consists of a slave robot that controls two active cannulas with grippers mounted at their tips, and a master console which allows teleoperation via two haptic interfaces. Vision is provided by a conventional endoscope, either manually operated or held by a fixed passive articulated arm.

A. Workspace Characterization

At Vanderbilt Medical Center, endonasal skull base surgery is typically performed through the surgically widened nasal passage of one nostril. To characterize the available workspace for surgery at the pititary gland, we used preoperative computed-tomography (CT) images of seven patients, processed using the open-source DICOM viewer OsiriX [31]. With assistance from experienced skull base surgeons, we manually segmented the area of the workspace in the frontal image series. The resulting working volume for endonasal skull base surgery of an average sized human head is shown in Fig. 3. We determined the dimensions of the workspace using SolidWorks, which are depicted in Fig. 4.

The resulting workspace for the active cannulas is restricted by the entry point through the nostril, which is approximately a rectangle of 16×35 mm. Towards the sphenoid sinus, the passage widens, both laterally and medially, until it reaches the pituitary gland, which is the posterior part of the workspace. The distance from the nostril entrance to the pituitary is about 10 cm, and the pituitary can be approximated by an ellipsoid with an 8.5 mm major radius and a 6 mm minor radius.

Concentric tube robots can be custom designed for specific application requirements. Parameters that may be selected include the number of tubes, tube diameter and stiffness, and

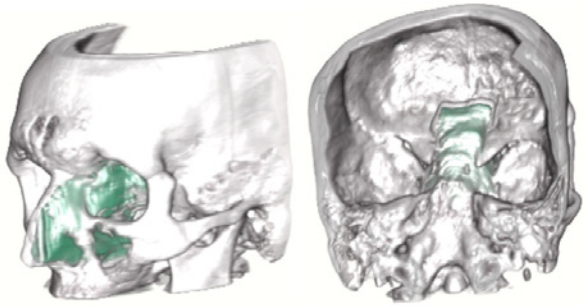

Fig. 3: Maximum workspace (green) through one nostril for endonasal skull base surgery on an average sized human.

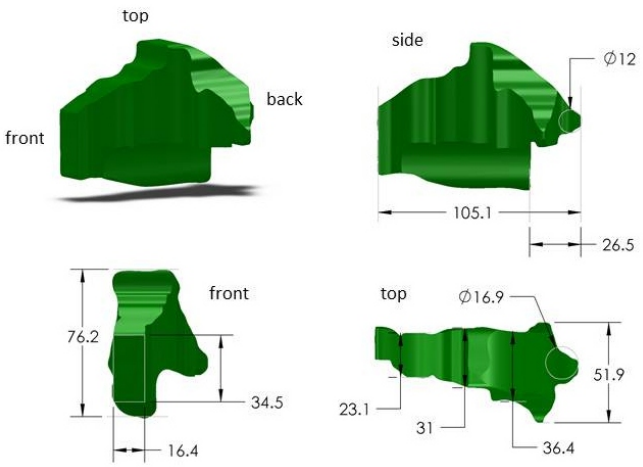

Fig. 4: Working volume dimensions (in mm). The upper left volume view corresponds to left view in Fig. 3

the precurved shape of each tube. A suitable actuation unit must also be built to grasp tube bases and apply desired translational and rotational displacements to them. In the following Sections, the design of our system is described in detail.

B. Concentric Tube Tool Shaft Architecture

Concentric tube robots provide a central working channel, which can accommodate any kind of end-effector which can be inserted through the innermost tube. In our prototype system, we use modified flexible grasping forceps (EndoJaw, FB-211K, Olympus, Japan). This was accomplished by removing the EndoJaw's outer sheath and replacing it with a concentric tube robot. The grippers are actuated by two thin tendons that travel through the cannula's inner tube. The diameter of the stainless steel forceps is 1.4 mm. Fig. 5 depicts a concentric tube robot with attached gripper.

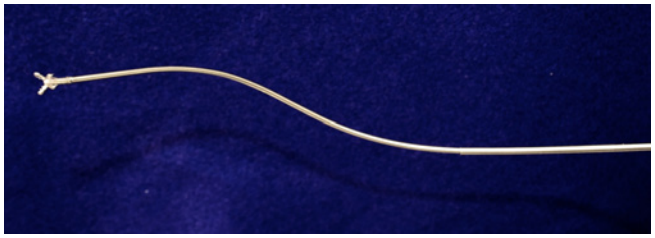

Fig. 5: Concentric tube robot with grasping forceps.

C. Optimized Active Cannula Design

As mentioned previously, the concentric tube architecture permits many design parameters to be selected to match application requirements. As an illustration of how this may be accomplished, we conducted the following study to determine suitable cannula tube parameters for pituitary surgery. Here, we restrict ourselves to considering cannulas constructed of tubes that have an initial straight section at their bases, followed by a curved section (with constant curvature) at their tips. For this special case the design parameters consist of the curvature of each tube and the lengths of the straight and curved portions of each tube.

We first discretized the workspace segmented in Sec. III-A, dividing it into areas where reachability is required (i.e. the pituitary gland), and into areas through which the cannula must simply pass (e.g. the nasal passage) on its way to the pituitary gland. Deriving an optimal active cannula design from a discrete workspace formulation is a combinatorial optimization problem, spanning a large parameter space. In this illustrative example, we selected a three-tube cannula (though we note that in future studies, the number of tubes, and non-circular tube precurvatures introduce additional optimization parameters). In view of the long, essentially straight entrance through the nasal cavity we assigned the outer tube to be straight with no curved section and with a length of 100 mm. We then optimized the middle and inner tubes over the parameters $\Phi = [l_{2s}, l_{2c}, k_2, l_{3s}, l_{3c}, k_3]$ with l_{is} being the straight lengths, l_{ic} being the curved lengths and k_i being the curvature values of tube i with tube 1 being the outermost tube and tube n the innermost.

Algorithm 1 Objective Function $f(\Phi)$ for optimal cannula tube design

Require: Ellipsoid E with radii (a, b, c)
Require: $[x_0, y_0, z_0]$ position of E
  $V_E = {}^4/_{3\pi abc}$
  list = NULL;
  for $\forall$ discrete actuator positions q **do**
    p_{tip} = ForwardKinematics(q,Φ)
    if $\left((\frac{p_{tip}(x)-x_0}{a})^2 + (\frac{p_{tip}(y)-y_0}{b})^2 + (\frac{p_{tip}(z)-z_0}{c})^2 \right) \leq 1$ **then**
      list.append(p_{tip})
    end if
  end for
  hull $= H_{convex}(\forall p \in list)$
  $V_c = V(hull)$
  return $1 - {}^{V_c}/_{V_E}$

As a tube design objective function to minimize, we took the percentage of the pituitary gland volume (an ellipsoid E of volume V_E – see Sec. III-A), which is not reachable by the cannula design Φ. To determine the reachable volume of cannula design Φ, we discretized the configuration space q in 3 mm translational steps and 45° rotational steps, and ran a torsionless forward kinematic cannula model [32] for each combination of discrete actuator values. Each cannula tip position which lies within the desired working volume E is stored in a list. Afterwards, the volume of the convex hull of all cannula tip positions within E is determined and divided by the volume V_E to form the objective function. The objective function $f(\Phi)$ is given in pseudo-code notation in Algorithm 1. The optimal cannula tube parameters are then derived by finding the minimum of the multivariable function f applying the unconstrained nonlinear simplex search method implemented in Matlab's `fminsearch`.

We determined the cannula tube parameters in Table I for the ellipsoid discussed in Section III-A. The saggital center plane of the optimized cannula workspace is depicted in Figure 6.

D. Actuation Unit Design

We designed a robotic actuation unit to coordinate the motion of all the tubes (axial rotation and translation at tube bases) in the bimanual active cannnula system. Fig. 7 shows the prototype. In order to actuate these degrees of freedom, there is an individual carrier for each tube which contains

TABLE I: Optimized tube parameters.

	Tube 1	Tube 2	Tube 3
Straight Length (mm)	100	120.9	164.4
Curved Length (mm)	0	60.2	60.6
Curvature (mm^{-1})	0	0.0084	0.0185
Inner Diameter (mm)	2.8	2.04	1.4
Outer Diameter (mm)	3.05	2.29	1.65

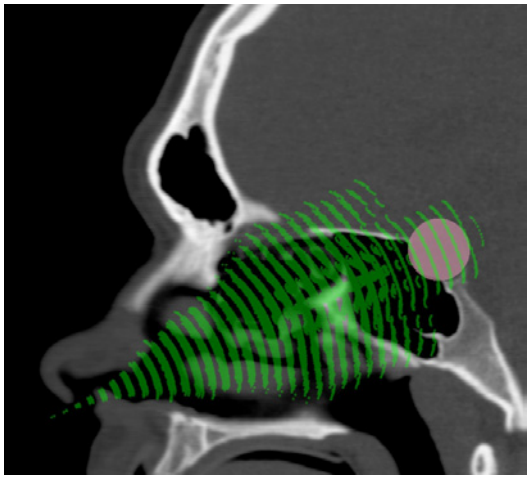

Fig. 6: Sagittal CT image with overlaid optimized cannula workspace (green). The pituitary gland is marked by a sphere.

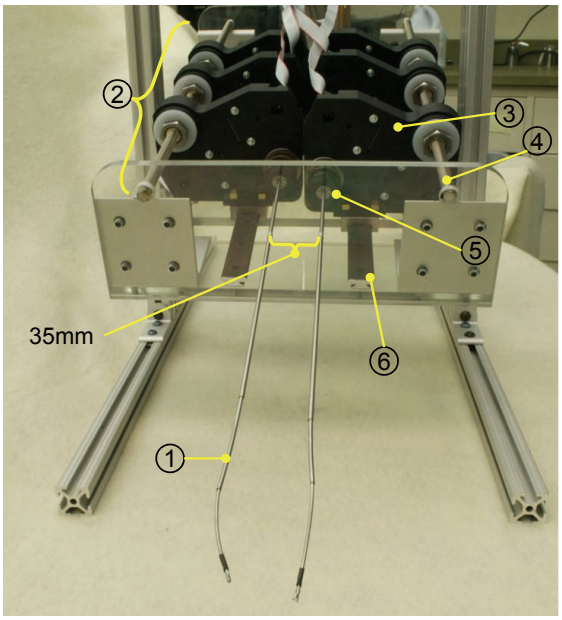

Fig. 7: Prototype bimanual active cannula robot. (1) Active cannula with gripper. (2) Actuation module for one cannula. (3) Carrier associated with one tube. (4) Lead screw for translation of the carriers. (5) Collet closure for grasping a tube. (6) Guide rail.

two encoded motors (RE 339152, Maxon Inc., Switzerland). These were selected based on a desired maximum torque of 0.25 Nm and translational speed of 4 cm/s for teleoperation (torque and speed requirements were qualitatively determined). On a given carrier, translation is accomplished by one motor using a worm gear to spin a nut that rides on a stationary lead screw. The rotation mechanism on a given carrier also uses a worm gear to spin the spring collet used to grasp the base of its respective tube. Use of a collet closure system permits easy replacement of tubes or changes in tube diameters as needed.

The carriers are affixed to a frelon self-lubricating guide block that rides on an aluminum guide rail. For each three tube active cannula, three carriers ride on a single guide rail, making up one actuation module. In this design, we have mirrored two modules and placed them next to each other. Two disposable biopsy forceps (see Section III-B) were inserted through the innermost tube to use as end effectors. Each actuation module is controlled by a separate control board (DMC-4080, Galil, USA) that provides low level PID control and amplification, and enables interfacing via Ethernet.

E. Teleoperation

We utilize two master Phantom Omni devices (Sensable, Wilmington, USA) to teleoperate the two active cannulas. Both devices are interfaced with IEEE-1394a Firewire. The user operates the stylus and starts/stops the teleoperation by pressing/releasing a button on the stylus. The stylus tip frame (position and orientation) at the start of the teleoperation is set as the teleoperation coordinate frame and all subsequent stylus frames are reported with respect to that coordinate system. This allows us to directly map between the master and slave frames, and enables "clutching" to recenter the master if desired.

In order to determine the actuator values (rotations and translations of the tubes bases) that will produce the desired end-effector poses, our approach adapts differential-inverse-kinematics strategies, since we can obtain forward kinematics solutions and manipulator Jacobians J at rates sufficient for teleoperation [33]. In particular, we adapted a generalized damped-least-squares approach to the differential-inverse-kinematics problem [34], [35]. The actuator velocities are determined by minimizing a custom objective function which primarily takes into account the trajectory tracking accuracy, and secondary objectives as stability, actuator velocity limits and avoidance of actuator limits and singular configurations. The objective function is defined as

$$F = \underbrace{(J\dot{q} - v_0)^T W_0 (J\dot{q} - v_0)}_{\text{Weighted Tracking Accuracy}} + \sum_{i=1}^{m} \underbrace{(\dot{q} - v_i)^T W_i (\dot{q} - v_i)}_{\text{Damping \& Avoiding}},$$

where v_0 is the desired end-effector velocity vector, m the number of secondary objectives, v_i are desired actuator velocity vectors set to either zero to achieve damping or to an objective function penalizing closeness to undesirable configurations, and W_i are non-negative symmetric weighting matrices which are either constant or configuration dependent. The actuator velocities $\dot{q}$ minimizing our objective function can be obtained as

$$\dot{q} = \left(J^T W_0 J + \sum_{i=1}^{m} W_i \right)^{-1} \left(J^T W_0 v_0 + \sum_{i=1}^{m} W_i v_i \right).$$

IV. PROOF OF CONCEPT CADAVER STUDY

To determine clinical feasibility we evaluated our system in a cadaver study. The nasal passages were surgically prepared, the sphenoid sinus exposed, and the anterior wall

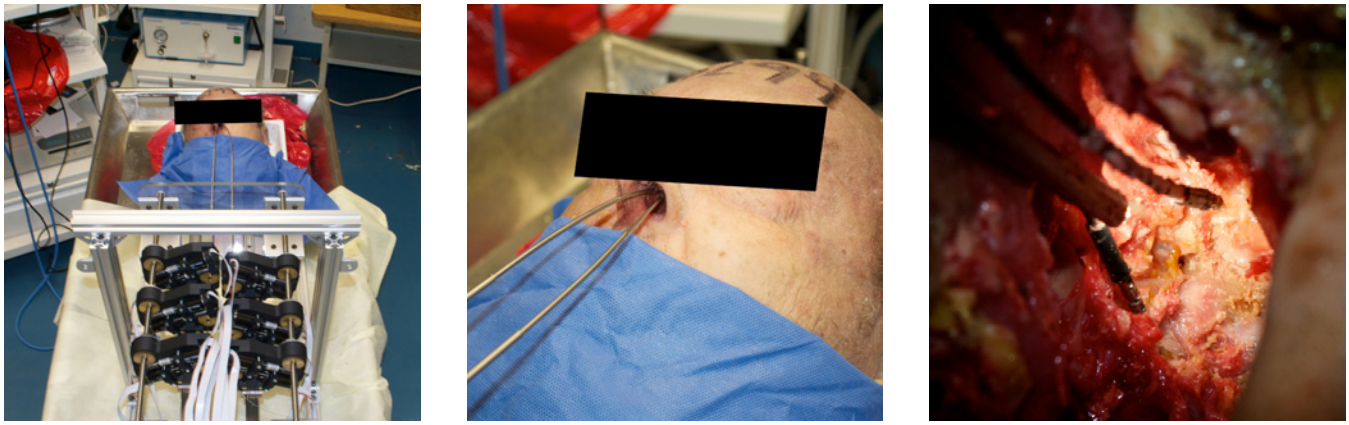

(a) (b) (c)

Fig. 8: Proof of concept cadaver study. (a) System setup in cadaver head study. (b) The two cannula robots enter through one nostril. (c) Sagittal view onto surgical site. The endoscope and the two robot arms are shown approaching the frontal wall of the pituitary gland.

of the pituitary gland opened. The head was situated on the operating table in the typical position used in endonasal surgery.

We constructed a positioning stage for the robot from aluminum profiles (80/20 Inc.). The robot was situated on the operating table in a relative angle of approximately 45 ° to the head. A straight rigid endoscope with 4 mm diameter and a view angle of 30 ° was manually inserted through the nostril and manually maintained in position. Both robotic arms were inserted through the right nostril and could reach the pituitary gland while maintaining maneuverability. Fig. 8 shows the experimental setup and Fig. 9 shows an intraoperative image of the endoscopic view onto the pituitary gland.

In order to fully observe the instrument tips and endoscope, a dissection of the left facial compartment from the nasal septum was performed. The view inside the skull base was offered through the dissection. The sagittal view onto the surgical site is shown in Fig. 8c.

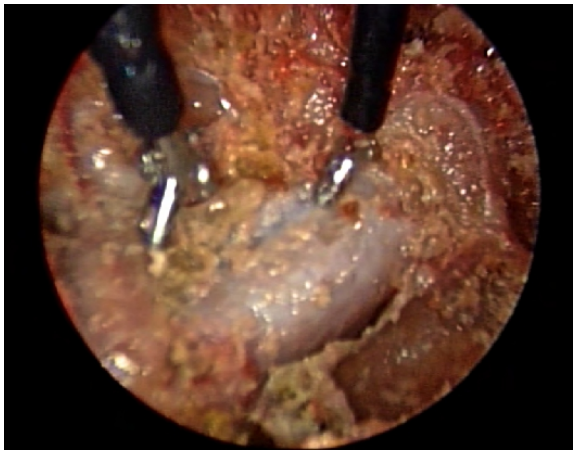

Fig. 9: Intraoperative endoscope view onto the pituitary gland in cadaveric study.

V. CONCLUSIONS AND FUTURE WORK

The high incidence of skull base tumors and the invasiveness of traditional transcranial and transfacial approaches provides strong motivation for an endonasal approach. The constrained nasal access path through which multiple rigid manual instruments must work makes the manual procedure challenging even for expert surgeons and time intensive to learn, motivating a robotic approach. The use of curved, tentacle-like manipulators in such a robotic system is desirable because it offers the promise of reaching locations inaccessible to straight tools, making better use of preoperative image information for guidance, and reducing the quantity of healthy tissue that must be removed to achieve adequate access to the surgical field.

In this paper we described the design of a prototype system for bimanual teleoperated endonasal skull base surgery. Primary contributions of the current work include our description of the surgical procedure, geometric characterization of the workspace, system design concept, and demonstration of concept in a cadaver experiment. Other contributions in this paper (including mechanical design, our optimization algorithm, and our teleoperation algorithm) are illustratory in nature. We include them not as complete and definitive treatises on the various topics, but rather to illustrate the many open research questions that have been posed during our initial system development and application studies. Each of these topics, as well as implementation of various forms of robotic assistance using image guidance, provide avenues to enhance the system we have described and to endow it with new capabilities.

There are also many other foreseeable applications for a teleoperated robotic surgical assistant with needle-diameter tentacle-like manipulators, including enhancing surgical interventions in the middle ear, throat, other neural spaces besides the skull base, and even in fetal surgery. In the abdomen, incisions or punctures less than 3 mm in diameter typically heal without any scaring whatsoever, making a sys-

tem like the one we describe potentially much less invasive than standard minimally invasive (i.e. done through 5-12 mm trocars) laparoscopic or single port (i.e. all tools inserted through a single, larger port) surgical approaches. Thus, we provide the results in this paper not only as a description of a specific system developed, but also as an illustration of an emerging paradigm in robotic surgery that we believe promises to improve outcomes in many future surgical and interventional procedures.

REFERENCES

[1] Y. S. Kwoh, J. Hou, E. A. Jonckheere, and S. Hayati, "A robot with improved absolute positioning accuracy for CT guided stereotactic brain surgery," *IEEE Transactions on Biomedical Engineering*, vol. 35, no. 2, pp. 153–160, 1988.

[2] R. H. Taylor, "A Perspective on Medical Robotics," *Proceedings of the IEEE*, vol. 94, no. 9, pp. 1652–1664, 2006.

[3] G. Dogangil, B. L. Davies, and F. Rodriguez y Baena, "A review of medical robotics for minimally invasive soft tissue surgery," *Proceedings of the Institution of Mechanical Engineers, Part H: Journal of Engineering in Medicine*, vol. 224, no. 5, pp. 653–679, 2010.

[4] A. Parmar, D. G. Grant, and P. Loizou, "Robotic surgery in ear nose and throat." *European Archives of Oto-rhino-Laryngology*, vol. 267, no. 4, pp. 625–33, 2010.

[5] U. Hagn, R. Konietschke, A. Tobergte, M. Nickl, S. Jörg, B. Kübler, G. Passig, M. Gröger, F. Fröhlich, U. Seibold, L. Le-Tien, A. Albu-Schäffer, A. Nothhelfer, F. Hacker, M. Grebenstein, and G. Hirzinger, "DLR MiroSurge: a versatile system for research in endoscopic telesurgery." *International Journal of Computer Assisted Radiology and Surgery*, vol. 5, no. 2, pp. 183–93, 2010.

[6] M. Miroir, J. Szewczyk, S. Mazalaigue, E. Ferrary, O. Sterkers, and A. B. Grayeli, "RobOtol: from design to evaluation of a robot for middle ear surgery," in *IEEE/RSJ International Conference on Intelligent Robots and Systems*, 2010, pp. 850–856.

[7] N. Simaan, K. Xu, A. Kapoor, W. Wei, P. Kazanzides, P. Flint, and R. Taylor, "Design and Integration of a Telerobotic System for Minimally Invasive Surgery of the Throat." *International Journal of Robotics Research*, vol. 28, no. 9, pp. 1134–1153, 2009.

[8] J. Ding, K. Xu, R. Goldman, P. Allen, D. Fowler, and N. Simaan, "Design, simulation and evaluation of kinematic alternatives for Insertable Robotic Effectors Platforms in Single Port Access Surgery," in *IEEE International Conference on Robotics and Automation*, 2010, pp. 1053–1058.

[9] A. Garg, R. C. Dwivedi, S. Sayed, R. Katna, A. Komorowski, K. A. Pathak, P. Rhys-Evans, and R. Kazi, "Robotic surgery in head and neck cancer: a review." *Oral Oncology*, vol. 46, no. 8, pp. 571–6, 2010.

[10] A. Arora, A. Cunningham, G. Chawdhary, C. Vicini, G. S. Weinstein, A. Darzi, and N. Tolley, "Clinical applications of Telerobotic ENT-Head and Neck surgery." *International Journal of Surgery*, vol. 9, no. 4, pp. 277–84, 2011.

[11] M. Kupferman, F. Demonte, F. C. Holsinger, and E. Hanna, "Transantral robotic access to the pituitary gland." *Otolaryngology–Head and Neck Surgery*, vol. 141, no. 3, pp. 413–5, 2009.

[12] B. W. O'Malley and G. S. Weinstein, "Robotic skull base surgery: preclinical investigations to human clinical application." *Archives of Otolaryngology–Head & Neck Surgery*, vol. 133, no. 12, pp. 1215–9, 2007.

[13] J. Wurm, T. Dannenmann, C. Bohr, H. Iro, and K. Bumm, "Increased safety in robotic paranasal sinus and skull base surgery with redundant navigation and automated registration," *International Journal of Medical Robotics and Computer Assisted Surgery*, vol. 01, no. 03, p. 42, 2005.

[14] M. Matinfar, C. Baird, A. Batouli, R. Clatterbuck, and P. Kazanzides, "Robot-assisted skull base surgery," in *IEEE/RSJ International Conference on Intelligent Robots and Systems*, 2007, pp. 865–870.

[15] T. Xia, C. Baird, G. Jallo, K. Hayes, N. Nakajima, N. Hata, and P. Kazanzides, "An integrated system for planning, navigation and robotic assistance for skull base surgery." *International Journal of Medical Robotics and Computer Assisted Surgery*, vol. 4, no. 4, pp. 321–30, 2008.

[16] C. Nimsky, J. Rachinger, H. Iro, and R. Fahlbusch, "Adaptation of a hexapod-based robotic system for extended endoscope-assisted transsphenoidal skull base surgery." *Minimally Invasive Neurosurgery*, vol. 47, no. 1, pp. 41–6, 2004.

[17] P. Dupont, J. Lock, and B. Itkowitz, "Real-time position control of concentric tube robots," in *IEEE International Conference on Robotics and Automation*, 2010, pp. 562–568.

[18] D. C. Rucker, R. J. Webster III, G. S. Chirikjian, and N. J. Cowan, "Equilibrium Conformations of Concentric-Tube Continuum Robots," *International Journal of Robotics Research*, vol. 29, no. 10, pp. 1263–1280, 2010.

[19] D. C. Rucker, B. A. Jones, and R. J. Webster III, "A Geometrically Exact Model for Externally Loaded Concentric-Tube Continuum Robots," *IEEE Transactions on Robotics*, vol. 26, no. 5, pp. 769–780, Oct. 2010.

[20] P. E. Dupont, J. Lock, B. Itkowitz, and E. Butler, "Design and Control of Concentric-Tube Robots." *IEEE Transactions on Robotics*, vol. 26, no. 2, pp. 209–225, 2010.

[21] J. a. F. Nogueira, A. Stamm, and E. Vellutini, "Evolution of endoscopic skull base surgery, current concepts, and future perspectives." *Otolaryngologic Clinics of North America*, vol. 43, no. 3, pp. 639–52, 2010.

[22] "American Brain Tumor Association (ABTA)," 2011. [Online]. Available: http://abta.org

[23] P. Cappabianca, *Cranial, craniofacial and skull base surgery*. Springer, 2009.

[24] C. H. Snyderman, H. Pant, R. L. Carrau, D. Prevedello, P. Gardner, and A. B. Kassam, "What are the limits of endoscopic sinus surgery?: The expanded endonasal approach to the skull base." *The Keio Journal of Medicine*, vol. 58, no. 3, pp. 152–60, 2009.

[25] L. M. Cavallo, F. Esposito, and P. Cappabianca, "Surgical limits in transnasal approach to opticocarotid region and planum sphenoidale: an anatomic cadaveric study." *World Neurosurgery*, vol. 73, no. 4, pp. 301–3, 2010.

[26] P. T. Russell and K. D. Weaver, "Anterior endoscopic skull-base surgery getting started: an otolaryngologist's perspective." *Current Opinion in Otolaryngology & Head and Neck Surgery*, vol. 15, no. 1, pp. 1–5, 2007.

[27] R. F. Labadie, B. M. Davis, and J. M. Fitzpatrick, "Image-guided surgery: what is the accuracy?" *Current Opinion in Otolaryngology & Head and Neck surgery*, vol. 13, no. 1, pp. 27–31, 2005.

[28] R. Balachandran, J. M. Fitzpatrick, and R. F. Labadie, "Accuracy of image-guided surgical systems at the lateral skull base as clinically assessed using bone-anchored hearing aid posts as surgical targets." *Otology & Neurotology*, vol. 29, no. 8, pp. 1050–5, 2008.

[29] J. K. Liu, L. D. Christiano, S. K. Patel, R. S. Tubbs, and J. A. Eloy, "Surgical nuances for removal of tuberculum sellae meningiomas with optic canal involvement using the endoscopic endonasal extended transsphenoidal transplanum transtuberculum approach." *Neurosurgical Focus*, vol. 30, no. 5, p. E2, 2011.

[30] J. J. Abbott, P. Marayong, and A. M. Okamura, "Haptic Virtual Fixtures for Robot-Assisted Manipulation," *Springer Tracts in Advanced Robotics*, pp. 49–64, 2007.

[31] A. Rosset, L. Spadola, and O. Ratib, "OsiriX: an open-source software for navigating in multidimensional DICOM images." *Journal of Digital Imaging*, vol. 17, no. 3, pp. 205–16, 2004.

[32] R. J. Webster, III, J. M. Romano, and N. J. Cowan, "Mechanics of Precurved-Tube Continuum Robots," *IEEE Transactions on Robotics*, vol. 25, no. 1, pp. 67–78, 2009.

[33] D. C. Rucker and R. J. Webster III, "Computing Jacobians and Compliance Matrices for Externally Loaded Continuum Robots," in *IEEE International Conference on Robotics and Automation*, 2011, pp. 945–950.

[34] C. Wampler, "Manipulator Inverse Kinematic Solutions Based on Vector Formulations and Damped Least-Squares Methods," *IEEE Transactions on Systems, Man, and Cybernetics*, vol. 16, no. 1, pp. 93–101, 1986.

[35] A. S. Deo and I. D. Walker, "Overview of damped least-squares methods for inverse kinematics of robot manipulators," *Journal of Intelligent & Robotic Systems*, vol. 14, no. 1, pp. 43–68, 1995.